

As an example of the range of effects to be expected, we have extended the approach used for SDS micelles to the smaller micelles of a similar surfactant, sodium octyl sulfate, for which the required data on aggregation number and density are available.<sup>16</sup> The calculated solubility in the core of these micelles is lower than for SDS by a factor of 4.1 on a mole fraction basis and 2.9 on a molar basis, whereas the surface area per unit volume is higher by a factor of 1.54. The net predicted decrease in  $K_m'$  is by a factor of 1.9.

For a more complete picture, however, it should be pointed out that, compared to benzene and other aromatic solutes for which the two-state model was originally proposed,<sup>3,4</sup> the highly polar nitroxide group with a large dipole moment of 3.14 D units is likely to be more sensitive to the specific nature of the micelle-water interfacial microenvironment. Thus, for benzene, the microenvironmental polarities in SDS and CTAC systems were found to be identical.<sup>3</sup> For both TEMPO and OTEMPO, significant differences between SDS and CTAC were found.<sup>2</sup> It seems, therefore, that the simple model of the micelle as an "oil drop" requires some modification for polar species such as nitroxides. The  $K_m'$  data of TEMPO in table I show some interesting differences in micelles of different charge types that are roughly consistent with trends in the transition energies and effective microenvironmental polarities reported.<sup>2</sup> Thus, considering the four C<sub>12</sub> surfactants,  $K_m'$  in SDS and Mg(DS)<sub>2</sub> are somewhat higher than in DM as expected from some extra stabilization of the nitroxide group in the oppositely or-

iented electric fields at the surface of these anionic micelles.<sup>2</sup> The probable increase in hydrogen-bonding interactions caused by the cations<sup>2</sup> is also in the right direction. In ZWIG 12, the dipole field is presumably aligned in the same direction as the nitroxide of TEMPO. It has been shown that this field causes some destabilization of the dipole, as reflected in the transition energy of TEMPO.<sup>2</sup> It should, therefore, decrease the value of  $K_m'$ , as observed. In view of the uncertainties of the data, these last few conclusions are considered to be tentative and need to be tested further in other systems. Some other unpublished microenvironmental studies do indicate some consistency with the points raised.<sup>18</sup>

The essential agreement of several approaches based on spectroscopic results<sup>2</sup> and on solution and surface thermodynamics indicates the usefulness of the two-state model of solubilization in micelles. Its extension to other kinds of lipid assemblies such as vesicles and membranes is highly desirable. The predominance of the adsorbed state of solubilized nitroxides indicates, as pointed out before,<sup>2-4,13</sup> that care should be exercised in using such molecules as spectroscopic sensors of microenvironments of hydrocarbon interiors of lipid assemblies.

*Acknowledgment.* This work was supported in part by the Public Health Science Research Grant GM-26078 and a fellowship to R.A.P. from the American Foundation for Pharmaceutical Education.

(18) Ramachandran, C.; Mukerjee, P., unpublished work.

## Computationally Simple Model for Multiphoton-Induced Chemical Processes

Richard J. McCluskey\* and S. V. Babu

Department of Chemical Engineering, Clarkson College of Technology, Potsdam, New York 13676 (Received: January 26, 1982; In Final Form: April 7, 1982)

A model for the multiphoton-induced decomposition of large polyatomic molecules that includes the effects of collisional deactivation is presented. Having only two adjustable parameters, the new model allows the time integral of the population of reactive energy states following the laser pulse to be computed very easily. The model is intended to describe experiments in which the bulk of reaction takes place after the laser pulse. It is particularly useful for describing decomposition through several competing reaction pathways. The model is applied to literature data on cyclobutanone. Very good agreement is obtained for the pressure dependence of the product ratio between the two decomposition channels and for the variation of the total decomposition with pressure for pressures less than about 0.6 torr. Reasons for the failure of the model at higher pressures are discussed.

### Introduction

Considerable activity in the area of laser-induced chemistry has amply demonstrated the feasibility of multiphoton absorption and its utility in isotope separation.<sup>1-3</sup> The enticing goal of bond-specific decomposition has largely proved to be elusive, and much current research is aimed at a methodical determination of kinetic models

for the multiphoton process. To this end, the investigation of multichannel reactions, in which a single substrate may react through several competing channels, has been of particular importance.<sup>4-9</sup> The relative yield between the different reaction pathways serves as an indicator of the

(1) V. S. Letokhov, *Annu. Rev. Phys. Chem.*, **28**, 133 (1977).  
 (2) R. V. Ambartzumian and V. S. Letokhov in "Chemical and Biochemical Applications of Lasers", Vol. III, C. B. Moore, Ed., Academic Press, New York, 1977, pp 167-316.  
 (3) J. I. Steinfeld in "Laser Induced Chemical Processes", J. I. Steinfeld, Ed., Plenum Press, New York, 1981.

(4) R. B. Hall and A. Kaldor, *J. Chem. Phys.*, **70**, 4027 (1979).  
 (5) O. M. Brenner, *Chem. Phys. Lett.*, **57**, 357 (1978).  
 (6) W. E. Farneth, M. W. Thomsen, and M. A. Berg, *J. Am. Chem. Soc.*, **101**, 6468 (1979).  
 (7) M. H. Back and R. A. Back, *Can. J. Chem.*, **57**, 1511 (1979).  
 (8) R. G. Harrison, H. L. Hawkins, R. M. Lee, and P. John, *Chem. Phys. Lett.*, **70**, 555 (1980).  
 (9) V. Starov, N. Selamoglu, and C. Steel, *J. Phys. Chem.*, **85**, 320 (1981).

time-averaged energy distribution over the microscopic states of the system.

The theory of unimolecular reactions induced by multiphoton absorption has been extensively developed for collision-free conditions.<sup>10-12</sup> Such conditions are usually encountered experimentally only in the case of molecular-beam studies or at very low pressures. Theory incorporating collisional effects is much more poorly developed, particularly for large polyatomic molecules.<sup>13</sup> Models proposed for describing collisional effects in multiphoton processes are elaborate and generally involve numerical solution of a large set of differential equations.<sup>9,14,15</sup>

This paper presents a new model for multiphoton-induced reactions which is computationally simple yet considers collisional deexcitation and accounts for some of the experimental observations. Some advantages of this model are that it utilizes information on intermolecular energy transfer obtained from chemical and photoactivation studies, that it has only two adjustable parameters and these have straightforward physical interpretation, that more sophisticated theories can be built readily into the model when deemed necessary, and, most significantly, that it gives insight into the phenomena most important for determining product yields.

Our incentive in developing the model is to describe laser-induced multichannel reactions that exhibit a strong pressure dependence. We have applied the model to data on the decomposition of cyclobutanone since this chemical system has been extensively studied<sup>7,8</sup> and sound data are available relating the extent of decomposition and the relative product yield to the pressure and the average energy absorption.<sup>9</sup> We find that the model predicts results which are in good agreement with these measurements.

### Assumptions in the Model

The phenomenon that we wish to analyze is the multiphoton chemistry occurring in experiments involving large polyatomic molecules and relatively short laser pulses. The assumptions in our model are listed below, and their applicability is discussed afterwards. (1) Reaction is described by RRKM theory. (2) Essentially all reaction occurs following the laser pulse. (3) Only a portion of the molecules within the beam volume interact with the radiation field, and there are a sufficient number of cold molecules present to quench the reaction rapidly by collisional deexcitation. (4) The internal energy distribution of excited molecules immediately following the laser pulse,  $f_0(E)$ , may be treated as known. (5) After the laser pulse, the temporal evolution of the energy distribution is determined primarily by reaction and by collision between vibrationally excited and vibrationally cold molecules. It is not strongly influenced by intermolecular energy exchange between high-energy molecules. (6) Collisional energy transfer probabilities are described by a stepladder model, where the probability for a transition from energy state  $E_i$  to energy state  $E_j$  is zero unless  $|E_i - E_j|$  is equal to the fixed value of the ladder's step size,  $\Delta E$ , and energy

transfer occurs on every collision.

### Discussion of the Assumptions

In general, multiphoton processes are extremely complicated. Molecules are simultaneously interacting with the radiation field, interacting with each other, and undergoing chemical reaction. To interpret these systems, it is convenient to deal with three time scales that characterize any experiment. These characteristic times are the effective laser pulse time,  $\tau_{\text{pulse}}$ , the mean time between any molecular collision,  $1/\omega'$ , and the mean time between strongly deexciting collisions,  $1/\omega$ . Since laser pulses are not square waves, reported pulse times should be viewed as upper bounds on  $\tau_{\text{pulse}}$ . Typical values for pulse times of CO<sub>2</sub> lasers are a few hundred nanoseconds or  $2 \times 10^{-7}$ – $4 \times 10^{-7}$  s. The mean time between collisions is the reciprocal of the collision frequency,  $\omega'$ , which may be calculated by using kinetic theory. There is uncertainty as to the proper temperature to employ in these calculations. Room temperature has been employed throughout this work because of the following: it is the only well-defined temperature in the experiment, it establishes an upper bound on  $1/\omega'$ , and it should describe approximately the population of cold molecules. The frequency of collision between a vibrationally excited and a cold molecule,  $\omega$ , is the total collision frequency,  $\omega'$ , multiplied by the fraction of cold molecules in the system. In experiments with large polyatomic molecules, the mean time between collisions at a pressure of 1 torr is about  $5 \times 10^{-8}$  s. A typical value cannot be given for the mean time between highly deactivating collisions since the fraction of cold molecules varies greatly depending on beam focus and geometry.

The first assumption is that the reaction rate and pathway are independent of the dynamics of the energy absorption process. It is a common assumption. There are some systems which exhibit non-RRKM behavior, but the majority of experiments lend support to the RRKM theory.<sup>16-18</sup> High-pressure chemical activation experiments place the time scale for intramolecular energy randomization at less than  $10^{-11}$  s, and, as noted above, the time scale of usual interest in multiphoton experiments is of the order  $10^{-7}$  s.<sup>19</sup>

Assumption 2, the absence of significant reaction during the laser pulse, is valid for all energy states in which a molecule's mean lifetime is greater than  $\tau_{\text{pulse}}$ . For assumption 2 to be useful, the population of energy states having mean lifetimes less than  $\tau_{\text{pulse}}$  must be small. This criterion can be expressed by the condition for

$$\tau_{\text{pulse}} = 1/k(E_r) \quad (1)$$

$$\int_{E_r}^{\infty} f_0(E) dE \approx 0 \quad (2)$$

where  $k(E)$  is the rate of reaction for a molecule with energy  $E$ ,  $E_r$  is the energy at which eq 1 is satisfied, and  $f_0(E)$  is the energy distribution of the "excited" molecules (see below, eq 5 or 8) following the laser pulse given the absence of reaction during the pulse. In general, the larger the substrate molecule, the more likely it is that the above criterion will be satisfied.

Operationally, if

(16) Aa. S. Sudbo, P. A. Schulz, E. R. Grant, Y. R. Shen, and Y. T. Lee, *J. Chem. Phys.*, **70**, 912 (1979).

(17) (a) J. T. Wanna and D. C. Tardy, *J. Phys. Chem.*, **85**, 3749 (1981); (b) J. C. Stephenson, S. E. Bialkowski, D. S. King, E. Thiele, J. Stone, and M. F. Goodman, *J. Chem. Phys.*, **74**, 3905 (1981).

(18) P. J. Robinson and K. A. Holbrook, "Unimolecular Reactions", Wiley-Interscience, New York, 1972.

(19) I. Oref and B. S. Rabinovitch, *Acc. Chem. Res.*, **79**, 166 (1979).

(10) S. Mukamel, *Adv. Chem. Phys.*, **47**, 509 (1981).

(11) (a) M. Quack, *J. Chem. Phys.*, **69**, 1282 (1978); (b) M. Quack, "Laser-Induced Processes in Molecules", K. Kompo and S. D. Smith, Eds., Springer-Verlag, West Berlin, 1979, pp 142-4.

(12) M. Quack, P. Humbert, and H. van der Bergh, *J. Chem. Phys.*, **73**, 247 (1980).

(13) C. C. Jensen, J. I. Steinfeld, and R. D. Levine, *J. Chem. Phys.*, **69**, 1432 (1978).

(14) R. B. Hall, A. Kaldor, D. M. Cox, J. A. Horsley, P. Rabinowitz, G. M. Kramer, R. G. Bray, and E. T. Maas, Jr., *Adv. Chem. Phys.*, **47**, 639-60 (1981).

(15) W. C. Danen and J. C. Jang in "Laser-Induced Chemical Processes", J. I. Steinfeld, Ed., Plenum Press, New York, 1981.

$$\tau_{\text{pulse}} < 1/\omega' \approx 1/\omega \quad (3)$$

the theory of collisionless interaction with the radiation field<sup>10-12</sup> may be applied during the laser pulse and the simpler equations of this paper utilized to describe subsequent reaction. In so doing,  $f_0(E)$ , will generally come from numerical solution of a master equation. We shall avoid this computational difficulty by use of assumption 2 to decouple interaction with the electromagnetic field from the chemical reaction process.

Assumption 3 is often made in current models of multiphoton absorption.<sup>9,20</sup> Several experiments have suggested a binodal energy distribution following a laser pulse. Our assumption is that there are two different populations of molecules following the laser pulse. One, which we call cold, contains most of the low-energy molecules. The form of this distribution is immaterial. We require only that it contain enough molecules to eliminate a long-time, "thermal" contribution to reactions of interest. The remaining molecules may be called the "excited" molecules.

Assumption 4 is admittedly an approximation. The energy distribution of the excited molecules following the laser pulse is unknown. However, its form should be intermediate to two established distributions, the Poisson and Boltzmann distributions.<sup>13</sup> In this paper we limit ourselves to a discussion of only these two distributions, both of which are determined by the mean energy of the excited population.

Under the condition

$$\tau_{\text{pulse}} < 1/\omega' \quad (4)$$

collisions should not perturb the energy distribution during the laser pulse. This implies that the energy distribution  $f_0(E)$  for the excited portion of the molecules is given by

$$f_0(E) = \sum_{n=0} f_B(E - nh\nu)\phi(n) \quad (5)$$

where  $f_B$  is the ambient Boltzmann energy distribution,  $\phi(n)$  is the normalized probability of absorbing  $n$  photons, and  $h\nu$  is the photon energy. If photon absorption is a Poisson process

$$\phi(n) = e^{-m} m^n / n! \quad (6)$$

where  $m$  is the average number of photons absorbed per excited molecule. Poisson distributions have been employed previously to describe, with success, laser-induced reactions.<sup>21</sup>

When the mean time between collisions is much less than the effective pulse time

$$1/\omega' \ll \tau_{\text{pulse}} \quad (7)$$

the excited molecules should be described approximately by an energy distribution of maximal entropy or Boltzmann form

$$f_0(E) = g(E)e^{-E/kT_{\text{eff}}} \quad (8)$$

where  $g(E)$  is the density of states function for energy  $E$ ,  $k$  is Boltzmann's constant, and  $T_{\text{eff}}$  is the temperature that endows the distribution with the correct mean energy.

We assume that the energy distribution of excited molecules at the end of the laser pulse is either a Poisson distribution, as expressed by eq 5 and 6, or a Boltzmann distribution, given by eq 8. These distributions have been compared in earlier work<sup>13</sup> and will be contrasted for cyclobutanone later in this paper. As pointed out above, the

true distribution is intermediate to these two limiting cases.

Assumption 5 is an approximation made to permit simplification of the analysis. Interaction between vibrationally hot molecules will cause them to move into or remain in a Boltzmann distribution. With increasing time the Boltzmann distributions, toward which the population of excited molecules strive, will have decreasing mean energy or temperature due to decomposition of the more energetic molecules and collision with vibrationally cold molecules.

The portion of the excited population that concerns us is that part with energy greater than the threshold energy for reaction. This leg or tail of the distribution will in time be depleted. If the excited population is in the form of a Boltzmann distribution at the end of the laser pulse, this depletion will be monotonic in time. However, if  $f_0(E)$  is a Poisson distribution, the population in the high-energy tail may initially increase in time as collisions between excited molecules move them into a broader, more Boltzmann-like distribution. Collision with cold molecules and decomposition will soon reverse this trend, and, after a time on the order of  $1/\omega$ , the high-energy tail will again be depleted monotonically in time.

Assumption 5 is that this monotonic depletion of the high-energy tail can be modeled satisfactorily as due to decomposition and collision with cold molecules. This is reasonable since the energy exchange in an encounter between an excited and a cold molecule is on average much larger than for collisions between two excited species. Furthermore, interaction between excited molecules will have two compensating effects. It will shift some molecules to higher energy to repopulate energy states depleted by reaction, and it will cause a gradual downshift in energy as the excited population cools. Assumption 5 will be more appropriate for systems with a large fraction of cold molecules, with large average energy transfer on collision with a cold molecule, and with small extent of reaction.

The stepladder model for collisional deexcitation has been shown to be suitable for describing results in a variety of chemical and photoactivation experiments.<sup>22-25</sup> It is a very useful one-parameter model that allows comparison with a large body of intermolecular energy transfer results. If the magnitude of the energy transfer occurring during a collision between excited and cold molecules is akin to that in chemical and photoactivation experiments, then the likelihood of the hot molecule gaining energy from the collision is very small and may be neglected. This is a key point in simplifying the calculation of the time integral of energy populations, and it will be discussed in detail.

The principle of detailed balance requires

$$P_{ij}g(E_j)e^{-E_j/kT} = P_{ji}g(E_i)e^{-E_i/kT} \quad (9)$$

where  $P_{ij}$  is the transition probability for changing from energy  $E_j$  to energy  $E_i$ ,  $g(E)$  is the density of states function, and  $T$  is the temperature of the population of cold molecules. For  $E_j < E_i$ , the ratio of the transition probabilities is

$$P_{ij}/P_{ji} = [g(E_i)/g(E_j)]e^{-\Delta E/kT} \quad (10)$$

Taking 298 K as descriptive of the cold population,  $\Delta E$  as  $1000 \text{ cm}^{-1}$  (12 kJ/mol), and the ratio of density of states functions as 3 (the maximum value that the ratio attains

(22) G. Kohlmaier and B. S. Rabinovitch, *J. Chem. Phys.*, **38**, 1692 (1963).

(23) R. Atkinson and B. A. Thrush, *Proc. R. Soc. London, Ser. A*, **316**, 131 (1970).

(24) R. J. McCluskey and R. W. Carr, Jr., *J. Phys. Chem.*, **82**, 2637 (1978).

(25) D. C. Tardy and B. J. Rabinovitch, *Chem. Rev.*, **77**, 369 (1977).

(20) A. C. Baldwin and J. R. Barker, *J. Chem. Phys.*, **74**, 3823 (1981).

(21) C. Reiser, F. M. Lussier, C. C. Jenson, and J. I. Steinfeld, *J. Am. Chem. Soc.*, **101**, 350 (1979).

for cyclobutanone at reactive energies), eq 10 gives the ratio of energy gain to energy loss transitions as only 0.024. This implies that neglect of energy gain on collision would change the number of molecules predicted to react by only a few percent.

### Mathematical Description of the Model

Based on the above assumptions, the "master equation" describing the time evolution of the reactive energy states is

$$dN_i/dt = -(k_i + \omega)N_i + \omega N_{i+\Delta E} \quad (11)$$

where  $N_i$  = (population with energy  $E_i$  at time  $t$ )/(population in  $f_0(E)$  at time zero),  $k_i$  = total decomposition rate constant for energy  $E_i$ ,  $\omega$  = collision frequency between an excited molecule and a vibrationally cold molecule, and  $\Delta E$  = average energy lost per collision. The above equation is subject to the initial condition that at  $t = 0$ , corresponding to the end of the laser pulse

$$N_i(t=0) = N_{i_0} = f_0(E_i) \quad (12)$$

This normalizes the initial population with respect to eq 5 or 8.

The general solution to eq 11 and 12 is

$$N_i(t) = e^{-(k_i+\omega)t} \left[ N_{i_0} + \int_0^t \omega N_{i+\Delta E} e^{(k_i+\omega)\tau} d\tau \right] \quad (13)$$

The instantaneous fractional decomposition is given by

$$D(t) = \sum_{E_i=E_0}^{\infty} k_i N_i(t) \quad (14)$$

and the observed fractional decomposition per pulse is

$$D = \int_0^{\infty} D(t) dt = \sum_{E_i=E_0}^{\infty} k_i \bar{N}_i \quad (15)$$

where  $\bar{N}_i$  is the time integral of the population with energy  $E_i$ , that is

$$\bar{N}_i = \int_0^{\infty} N_i(t) dt \quad (16)$$

and  $E_0$  is the threshold energy for decomposition.  $D$  represents the fraction of the population of excited molecules which decompose.

The  $k_i$  are obtained by using RRKM theory. In the case of competing parallel reaction pathways,  $k$  is the sum of the microscopic rate constants for each reaction. If there are only two decomposition pathways, a and b, the ratio of path a to path b decomposition is given by

$$D_a/D_b = \sum_{E_i=E_{0a}}^{\infty} k_{ia} \bar{N}_i / \sum_{E_i=E_{0b}}^{\infty} k_{ib} \bar{N}_i \quad (17)$$

where  $k_a$ ,  $E_{0a}$ ,  $k_b$ , and  $E_{0b}$  are the microscopic rate constants and threshold energies for reactions a and b, respectively.

The time integral of the population of energy states is eq 13 integrated over all time following the laser pulse. It can be shown to be

$$\bar{N}_i = \frac{1}{k_i + \omega} \left( N_{i_0} + N_{i+\Delta E} \frac{\omega}{k_{i+\Delta E} + \omega} + N_{i+2\Delta E} \frac{\omega}{k_{i+2\Delta E} + \omega} \frac{\omega}{k_{i+\Delta E} + \omega} + \dots + N_{i+L\Delta E} \prod_{j=1}^L \frac{\omega}{k_{i+j\Delta E} + \omega} \right) \quad (18)$$

This can be interpreted as the mean time that a molecule spends at energy  $E_i$  times the sum of the initial population of energy level  $i$  and of all higher energy levels weighted

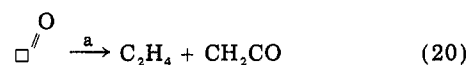
by the probability of molecules starting at those higher energies reaching level  $i$  without decomposing. In theory, the energy distribution given by eq 5 or 8 extends to infinite energy. In practice, the distribution may be terminated at an energy sufficiently high for the product of  $k_i$  and  $N_{i_0}$  to be negligible. The summation appearing in eq 18 is thus finite. It ends at the energy level  $i+L\Delta E$ , which may be thought of as the uppermost rung on an energy stepladder.  $\bar{N}_i$  is computed most easily through eq 19, and at the top of the energy stepladder  $\bar{N}_{i+\Delta E}$  is zero.

$$\bar{N}_i = \bar{N}_{i+\Delta E} \frac{\omega}{k_i + \omega} + \frac{N_{i_0}}{k_i + \omega} \quad (19)$$

The parameters to be specified are the fraction of molecules interacting with the laser field, the average number of photons absorbed by the excited molecules, and the average energy transfer per collision,  $\Delta E$ . The first two of these parameters are interrelated; one fixes the other. Furthermore, there are considerable data available from chemical and photoactivation experiments to aid in specifying the final parameter,  $\Delta E$ . Application of the model will be illustrated by using literature data on the multiphoton-induced decomposition of cyclobutanone.

### Application to Cyclobutanone Decomposition

Cyclobutanone undergoes decomposition via two reaction channels



The  $\text{C}_3\text{H}_6$  product is predominantly cyclopropane but includes the cyclic compound's isomerization product, propylene. The Arrhenius parameters for reactions a and b are<sup>9</sup>  $E_a = 217$  kJ/mol,  $A_a = 3.6 \times 10^{-14}$  s<sup>-1</sup>,  $E_b = 242$  kJ/mol, and  $A_b = 2.3 \times 10^{-14}$  s<sup>-1</sup>. Each reaction is believed to proceed through a biradical intermediate whose formation is rate limiting.<sup>26</sup> The vibrational frequency assignments used in RRKM models for these reactions are summarized in Table I. The microscopic rate constants are shown as a function of internal energy in Figure 1.

The collision number for bimolecular collisions between cyclobutanone molecules at room temperature was estimated by using a value of 6.6 Å for the collision diameter, a number intermediate to literature values of the collision diameter of cyclobutane and methylcyclobutane.<sup>28</sup> This was multiplied by the fraction of molecules not interacting with the radiation field to obtain the collision number for interaction between excited and cold molecules.

Starov et al.<sup>9</sup> provide excellent experimental data on cyclobutanone decomposition following a 0.3-μs CO<sub>2</sub> laser pulse at 1073.3 cm<sup>-1</sup>. Collimated-beam experiments were performed over the pressure range 0.2–10 torr with an approximately constant fluence of 3.2 J/cm<sup>2</sup>. The average number of photons absorbed per molecule,  $\langle n \rangle$ , within the path of the laser radiation was measured, although the accuracy of the measurement was poor at pressures below 1 torr. The percent decomposition per pulse and the relative yields of  $\text{C}_2\text{H}_4$  and  $\text{C}_3\text{H}_6$  products were determined over the investigated pressure range.

Evidence from chemical and photoactivation experiments on molecules excited to energies near 450 kJ/mol

(26) S. W. Benson and H. E. O'Neal, *Natl. Stand. Ref. Data Ser. (U.S., Natl. Bur. Stand.)*, 21 (1970).

(27) K. Frei and H. H. Gunthard, *J. Mol. Spectrosc.*, 5, 218 (1960).

(28) J. W. Simons, W. L. Hase, R. J. Phillips, E. J. Porter, and F. B. Growcock, *Int. J. Chem. Kinet.*, 7, 879 (1975).

TABLE I: RRKM Frequency Assignments for Cyclobutanone<sup>a</sup>

assignment	molecule, <sup>27</sup> cm <sup>-1</sup>	complex a, cm <sup>-1</sup>	complex b, cm <sup>-1</sup>
C-H	3021		
	3015		
	3011		
	2921		
	2919		
	2917		
C=O stretch	1977		
C-C=O	1612		
	1593		
CH <sub>2</sub> scissors	1515		
	1499		
	1455		
C-C stretch	1448	750	750
	1231		
	1192		
CH <sub>2</sub> rock	1151		
	1137		
	1059		
C-C stretch	975	750	750
	952	644	644
	881		
CH <sub>2</sub> rock	872	515	872
	823	340	340
	644	340	340
ring def	515	340	340
	340	150	150
	124	reaction coordinate	

<sup>a</sup> Geometric degeneracy factor = 2. Only the italicized frequencies are altered in the activated complexes.

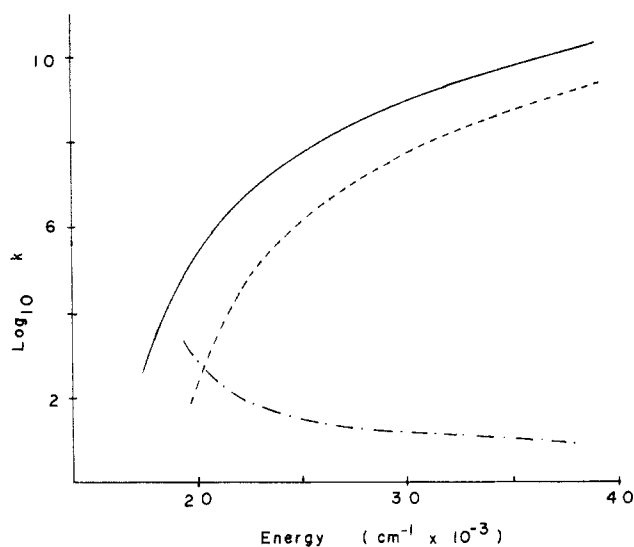


Figure 1. Logarithm of RRKM rate constants vs. energy for cyclobutanone decomposition:  $k_a$  in  $s^{-1}$  (—);  $k_b$  in  $s^{-1}$  (---); and  $k_a/k_b$  (-·-).

suggests that for a molecule as large as cyclobutanone the average energy transfer,  $\Delta E$ , in a collision with a cold molecule of equivalent size is between 10 and 40 kJ/mol.<sup>24</sup> Values of  $\Delta E$  over this range are considered in our calculations.

Calculations were performed by selecting a value of  $\Delta E$  and a pressure, through which  $\langle n \rangle$ , the experimental value of the average number of photons adsorbed by the entire irradiated volume, was fixed. A value of  $m$ , the average number of photons absorbed by the excited molecules, was then chosen, so as to hold  $\langle n \rangle/m$ , the fraction of molecules interacting with the laser field, constant. A more accurate choice requires the evaluation of the relative importance of rotational hole filling and V-T energy transfer collisions during the laser pulse. We return to this point later on

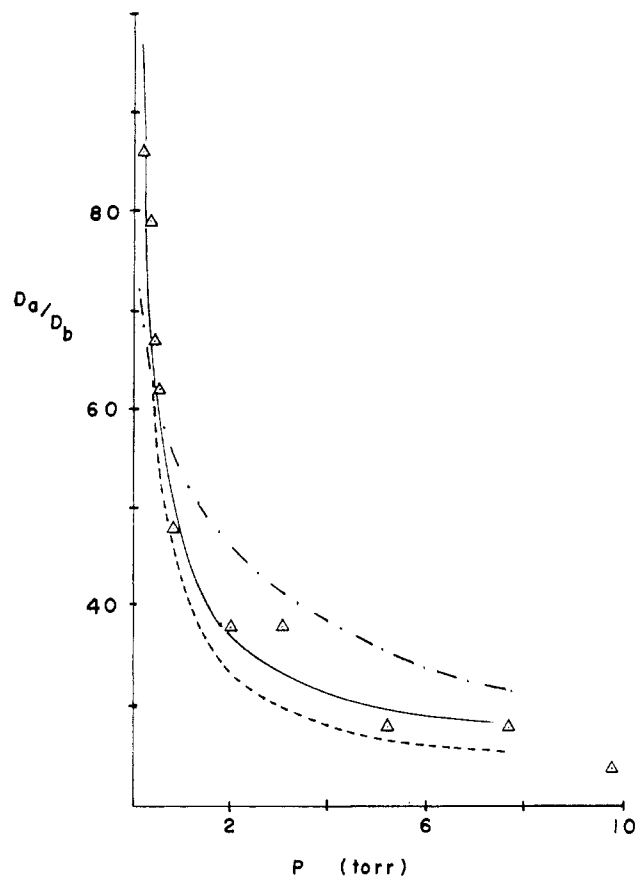


Figure 2. Relative reaction yield vs. pressure: experimental data ( $\Delta$ ); model of Starov et al. (-·-); proposed model with a Poisson distribution,  $\langle n \rangle/m = 0.70$ , and  $\Delta E = 1000 \text{ cm}^{-1}$  (—); proposed model with a Poisson distribution,  $\langle n \rangle/m = 0.70$ , and  $\Delta E = 3000 \text{ cm}^{-1}$  (---).

while discussing our results. The fraction of cold molecules within the irradiated volume at the end of the laser pulse is  $1 - \langle n \rangle/m$ . The frequency of collision between an excited and a cold molecule is found from eq 22, where  $1.9 \omega = [(1 - \langle n \rangle/m)(1.9 \times 10^7) \text{ s}^{-1} \text{ torr}^{-1}][P(\text{torr})]$  (22)

$\times 10^7$  is the collision frequency at 1 torr and 298 K. For calculations involving  $f_0(E)$  as a Boltzmann distribution, trial calculations were performed to establish the mean energy ( $1073m \text{ cm}^{-1}$ ) as a function of  $T_{\text{eff}}$ . This was a simple matter since, at the high temperatures involved, the mean energy is essentially a linear function of  $T_{\text{eff}}$ . Thereafter, for any desired  $m$  the appropriate value of  $T_{\text{eff}}$  was determined and used in eq 8 to give  $f_0(E)$ .

The overall computational procedure was to (1) calculate  $f_0(E)$  from eq 5 or 8, (2) calculate  $\bar{N}_i$  from eq 19, (3) obtain the relative yields from eq 17, and (4) obtain the percent decomposition per pulse by multiplying the result of eq 15 by  $\langle n \rangle/m$ . Further details of the computer calculations are found in an Appendix to this paper.

## Results

Some results of these calculations are presented in Figures 2 and 3. Figure 2 shows the ratio of decomposition by reaction 20 to that via reaction 21 plotted as a function of pressure. The experimental data are from Starov et al.<sup>9</sup> Calculated results are presented that employ average energy losses of 1000 and 3000  $\text{cm}^{-1}$ , 70% of the total population interacting with the laser field, and the Poisson form for  $f_0(E)$ , i.e., eq 5 and 6. Also shown are the results of a theoretical model proposed by Starov et al.<sup>9</sup> The superiority of the new model is evident. The results for  $\Delta E = 1000 \text{ cm}^{-1}$  fit the experimental data extremely well,

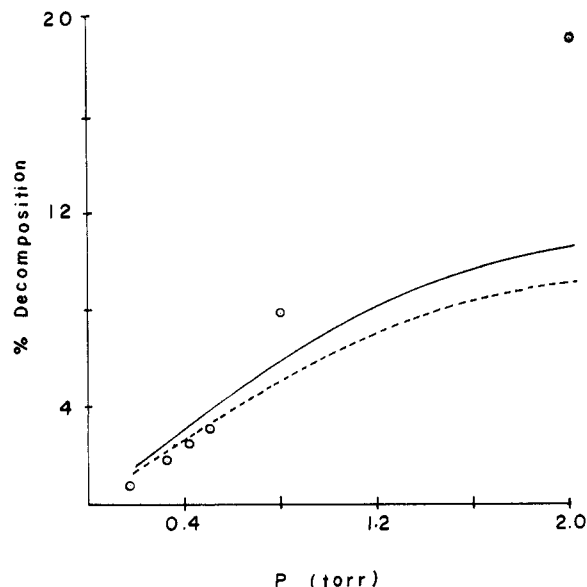


Figure 3. Percent decomposition per pulse within the irradiated volume vs. pressure: experimental data (O); proposed model with Poisson distribution,  $\langle n \rangle/m = 0.70$ , and  $\Delta E = 1000 \text{ cm}^{-1}$  (—); and the same model with  $\Delta E = 3000 \text{ cm}^{-1}$  (---).

TABLE II: Computational Results for the Poisson Distribution

$\langle n \rangle$	$m$	$P$ , torr	$\Delta E = 1000 \text{ cm}^{-1}$		$\Delta E = 3000 \text{ cm}^{-1}$	
			$D_a/D_b$	% decompn	$D_a/D_b$	% decompn
$\langle n \rangle/m = 0.65$						
9	13.8	0.51	55.8	5.39	50.9	4.67
11	16.9	2.0	33.1	13.5	30.4	11.6
12.1	18.6	7.7	24.6	16.1	22.5	13.4
$\langle n \rangle/m = 0.70$						
	11	0.18	100.7	1.44	91.9	1.27
	12	0.33	77.5	2.43	70.6	2.12
9	12.9	0.51	64.0	3.63	58.3	3.13
	14	0.80	51.9	5.89	47.3	5.06
11	15.7	2.0	37.9	9.70	34.5	8.21
12.1	17.3	7.7	27.6	12.0	25.2	9.83
$\langle n \rangle/m = 0.75$						
9	12	0.51	73.8	2.39	67.0	2.07
11	14.7	2.0	43.0	7.01	39.1	5.90
12.1	16.1	7.7	31.0	8.71	28.2	7.05
exptl						
		$P$ , torr	$D_a/D_b$		% decompn	
		0.18	86 ± 15		0.80 ± 0.06	
		0.33	70 ± 3		1.8 ± 0.1	
		0.51	62 ± 3		3.1 ± 0.2	
		0.80	48 ± 3		7.9 ± 0.7	
		2.0	38 ± 3		19 ± 4	
		7.7	28 ± 3		42 ± 1	

while those for  $\Delta E = 3000 \text{ cm}^{-1}$  are slightly low.

In Figure 3, the percent decomposition within the irradiated volume is plotted vs. pressure for pressures up to 2.0 torr. The experimental results of Starov et al. are compared with the same computational results illustrated in Figure 2. The model does not predict the relatively high extents of reaction observed at pressures above 0.6 torr. The experimental values increase sharply above this pressure. The match to experiments at lower pressures, where the percentage decomposition was below 5%, is reasonable.

More complete computational results are presented in Table II, for  $f_0(E)$  in a Poisson form, and in Table III, for

TABLE III: Computational Results for the Boltzmann Distribution

$\langle n \rangle$	$\langle E \rangle$ , $\text{cm}^{-1}$	$P$ , torr	$\Delta E = 1000 \text{ cm}^{-1}$			
			$D_a/D_b$	% decompn	$D_a/D_b$	% decompn
$\langle n \rangle/m = 0.80$						
9	12 060	0.51	56.5	2.82	62 ± 3	3.1 ± 0.2
11	14 840	2.0	35.1	7.13	38 ± 3	19 ± 4
12.1	16 230	7.7	26.4	8.47	28 ± 3	28 ± 3
$\langle n \rangle$	$\langle E \rangle$ , $\text{cm}^{-1}$	$P$ , torr	$\Delta E = 1000 \text{ cm}^{-1}$		$\Delta E = 3000 \text{ cm}^{-1}$	
			$D_a/D_b$	% decompn	$D_a/D_b$	% decompn
$\langle n \rangle/m = 0.85$						
9	11 300	0.51	65.9	2.08	59.5	1.85
11	13 780	2.0	40.1	5.23	36.6	4.57
12.1	15 300	7.7	29.2	6.94	26.6	5.88
$\langle n \rangle/m = 0.90$						
9	10 730	0.51			69.3	1.50
11	13 180	2.0			41.4	4.06
12.1	14 380	7.7			29.5	4.62

$f_0(E)$  as a Boltzmann distribution. Experimental results of Starov et al.<sup>9</sup> are given in both tables for ease of comparison. Table II contains data for excited molecules comprising 65%, 70%, and 75% of the total population, and for energy step sizes of 1000 and 3000  $\text{cm}^{-1}$ . For  $\langle n \rangle/m = 0.65$ , the relative yield calculations are consistently low for both step sizes, while the low-pressure values of percent decomposition are higher than observed experimentally. At  $\langle n \rangle/m = 0.70$ , the relative yield values for  $\Delta E = 1000 \text{ cm}^{-1}$  match the experimental values quite well, and at  $\Delta E = 3000 \text{ cm}^{-1}$  are low by a small amount. The percent decomposition results are slightly above experimental low-pressure values for both step sizes. This set of calculations is plotted in Figures 2 and 3. The final  $\langle n \rangle/m$  ratio, 0.75, gives low-pressure decomposition percentages that are low and yield ratios that are consistently high, though the 3000- $\text{cm}^{-1}$  step-size results are only slightly so. The data suggest that fine tuning of the  $\langle n \rangle/m$  ratio and  $\Delta E$  values could produce matches to the experimental results even better than those illustrated in Figures 2 and 3.

Calculations using  $f_0(E)$  as a Boltzmann distribution are summarized in Table III. A good fit to the experimental yield ratios is achieved at an  $\langle n \rangle/m$  ratio of 0.85, although the corresponding percent decomposition results are significantly less than those experimentally observed, even at low pressures. Calculations performed assuming excited-molecule mole fractions of 0.80 and 0.90 are also presented. At 0.80, the lowest step size considered,  $\Delta E = 1000 \text{ cm}^{-1}$ , gives relative yields that are slightly low. At 0.90, the  $\Delta E = 3000 \text{ cm}^{-1}$  results for the relative yields are slightly high. It is apparent that, for  $\Delta E$  values between 1000 and 3000  $\text{cm}^{-1}$ , the experimental relative yields can be matched only for  $\langle n \rangle/m$  values close to 0.85 where the corresponding percent decomposition results will be below experimental values. Agreement with both the experimental  $D_a/D_b$  ratio and the low-pressure percent decomposition could probably be achieved by considering smaller-energy step sizes, but this would mean having to consider up transitions and would not be consistent with chemical and photoactivation results.

#### Comparison of the Poisson and Boltzmann Distributions

What we have been calling the Poisson form for  $f_0(E)$  is really a convolution of a room-temperature Boltzmann

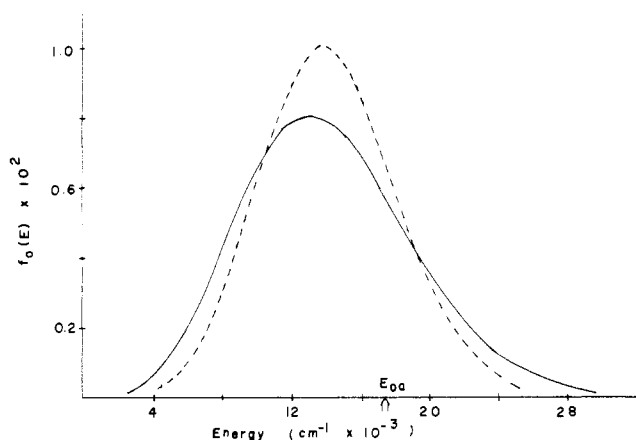


**Figure 4.** Energy distribution following the laser pulse: Poisson distribution (---) and Boltzmann distribution (—).

distribution with a Poisson distribution. As a consequence, the distribution function given by eq 5 is not smooth but has a series of sharp spikes at intervals corresponding to the photon energy ( $1100\text{ cm}^{-1}$ ). To allow a better comparison with a high-temperature Boltzmann distribution, the  $f_0(E)$  from eq 5 for  $m = 13$  photons was averaged over  $1100\text{-cm}^{-1}$  intervals. The resulting distribution is compared with a  $1540\text{ K}$  Boltzmann distribution in Figure 4. Both distributions have mean energies of  $172\text{ kJ/mol}$  ( $14\,300\text{ cm}^{-1}$ ). The distributions are shown as continuous curves even though they were discretized in  $100\text{-cm}^{-1}$  steps for all of our calculations.

The Poisson form of the distribution function is slightly narrower than the Boltzmann distribution with the same mean energy. The consequences of this can be recognized by comparing those portions of the distributions above the reaction threshold energy with the energy dependence of the microscopic rate constants shown in Figure 1. Figure 4 shows that the Boltzmann distribution has a smaller population close to the threshold energy and a larger population at energies above  $20\,000\text{ cm}^{-1}$ . The ratio of rate constants plotted in Figure 1 illustrates that the greatest reaction path selectively is achieved at energies close to the threshold energy and that the least selectivity is found at high energies. The Poisson form of  $f_0(E)$  therefore leads to higher  $D_a/D_b$  ratios than the Boltzmann distribution at the same mean energy. To achieve a high value of reaction selectivity,  $D_a/D_b$ , with the Boltzmann distribution, the population of high-energy states must be reduced by shifting the distribution to a lower mean energy. But, as seen from the data in Table III, this brings down the percent decomposition to a value below that obtained experimentally. The important point is that small differences in the high-energy tail of different forms for  $f_0(E)$  cause major variation in predicted values of  $D_a/D_b$  ratio and percent decomposition.

### Discussion of Results

Our computationally simple model of multiphoton-induced dissociation through competitive reaction pathways has been applied successfully to the experimental data of Starov et al. on cyclobutanone. The model gives an excellent match to the variation in reaction selectivity,  $D_a/D_b$ , with change in pressure. It also gives a reasonable representation of the overall percentage decomposition for extents of reaction below 5% (pressures below 0.6 torr). It fails to predict the markedly higher percentage decompositions that were observed in experiments at pressures above 0.6 torr. This is not surprising, since the model is not expected to apply to systems of excited molecules with

high mean energy and large extents of reaction. The failure of both assumption 3, that there are an adequate number of cold molecules to quickly quench the reaction, and assumption 5, that repopulation of high-energy states by collision between hot molecules can be ignored, is anticipated under these conditions.

$E_0$ , defined by eq 1, can be estimated from Figure 1 as  $22\,000\text{ cm}^{-1}$  for a laser pulse time of 300 ns. The integral appearing in eq 2 has a value of only 0.043 for the Poisson distribution illustrated in Figure 4, that is, with  $m = 13$  photons. However, for  $m = 17$  photons, the value utilized in high-pressure calculations for  $\langle n \rangle/m = 0.70$ , this integral has a magnitude of 0.26. This implies the breakdown of assumption 2. The ability of the model to predict the correct  $D_a/D_b$  even under these conditions evidently arises from a consistent undercount of decomposition from both the high- and low-energy reactive states.

The calculated results are much more sensitive to  $f_0(E)$ , the energy distribution following the laser pulse, than to  $\Delta E$ , the average energy transfer in a strongly deenergizing collision. For both Boltzmann and Poisson distributions, variation of the energy transfer step size from  $1000$  to  $3000\text{ cm}^{-1}$  causes only a 10% decrease in both the  $D_a/D_b$  ratio and the total extent of decomposition. In contrast, a change in the average energy of the excited population from  $13\,800$  to  $14\,800\text{ cm}^{-1}$  causes the reaction selectivity to drop from 40 to 35 but the overall extent of reaction increases by 37%.

The results obtained by using the Poisson form (eq 5) for  $f_0(E)$  give a better match to the experimental values of  $D_a/D_b$  and percent decomposition than do results calculated by using a Boltzmann distribution for  $f_0(E)$ . This implies that the model gives a more realistic estimate of  $N_i$ , the time integral of the population of energy states, with the use of eq 5 rather than eq 8 for  $f_0(E)$ . It does not imply that the excited molecules never achieve a Boltzmann-like energy distribution.

In the presentation of our results we have taken  $\langle n \rangle/m$ , the fraction of molecules interacting with the laser pulse, as independent of pressure. The dominant collisional mechanisms affecting  $\langle n \rangle$  and  $m$  are rotational hole filling which would cause  $\langle n \rangle/m$  to increase and V-T transfer collisions which allow a molecule to recycle through absorption transitions and may decrease  $\langle n \rangle/m$ .<sup>29,30</sup> In systems containing an inert collider rotational hole filling should dominate over V-T collisions. However, in the pure cyclobutanone experiments that we have analyzed, V-T collisions should be highly effective, so the net change in  $\langle n \rangle/m$  with pressure is uncertain. Allowing the  $\langle n \rangle/m$  ratio to decrease with pressure would permit a better fit to the percent decomposition data at higher pressures and also allow a better fit to the  $D_a/D_b$  results with the Boltzmann form for  $f_0(E)$ .

Our simple mathematical model can still be used with systems in which rotational hole filling is sufficiently important to mandate an increase in  $\langle n \rangle/m$  with increasing pressure. Equations 15–19 are independent of how the  $\langle n \rangle/m$  ratio is specified.

The greatest asset of our proposed model lies in the ease with which the time integral of the population of energy states may be found. The derivation of these populations is certainly not rigorous. But the assumptions on which the model is based are reasonable, and the accuracy of

(29) G. P. Quigley and J. L. Lyman in "Laser Induced Processes in Molecules", K. L. Kompa and S. D. Smith, Ed., Springer-Verlag, West Berlin, 1979, p 134.

(30) J. Stone, E. Thiele, M. F. Goodman, J. C. Stephenson, and D. S. King, *J. Chem. Phys.*, 73, 2259 (1980).

approximation is enhanced by compensating effects. We feel it is remarkable that what is essentially a one-parameter model ( $\Delta E$  can be estimated from chemical and photoactivation data and results are not highly sensitive to it) can predict the pressure dependence of both the reaction selectivity and the extent of decomposition, albeit restricted to low yields.

### Conclusions

The new model for multiphoton-induced chemistry is successful in describing the pressure dependence of the reaction selectivity and the percent decomposition for reaction yields below 5% for the decomposition of cyclobutanone in a collimated beam of CO<sub>2</sub> laser with fluence of approximately 3.2 J/cm<sup>2</sup>. The model fails to predict correctly the percentage decomposition experimentally observed under conditions such that the reaction yield is greater than 5%.

The model suggests that for systems similar to cyclobutanone the reaction selectivity and yield are more sensitive to the energy distribution following the laser pulse than to the dynamics of the collisional deexcitation process.

### Appendix

*Details of the Computational Procedures.* Density of states functions were computed by using the Beyer-Swinehart exact count algorithm<sup>31</sup> and the fundamental vibrational frequencies of cyclobutanone given in Table I. Boltzmann distributions were obtained from these and discretized in 100-cm<sup>-1</sup> intervals. The distribution func-

(31) T. Beyer and D. F. Swinehart, *Commun. A.C.M.*, 16, 379 (1973).

tions describing the population of excited molecules were taken as Boltzmann or calculated by using eq 5. The photon energy was rounded from 1073 to 1100 cm<sup>-1</sup> for eq 5. The distribution functions were computed up to an energy of at least 49 400 cm<sup>-1</sup> (590 kJ/mol).

The sums of states for each activated complex described in Table I were also computed by using the Beyer-Swinehart algorithm. RRKM rate constants were determined at 100-cm<sup>-1</sup> intervals above the threshold energies of 17 400 and 19 600 cm<sup>-1</sup> for reactions 20 and 21, respectively.

These rate constants and the above-mentioned distribution functions,  $f_0(E)$ , were used in eq 12 and 19 to determine the time integral of the state population,  $\bar{N}_i$ . The highest energy considered in these calculations was always at least 37 400 cm<sup>-1</sup>. Trial calculations demonstrated that inclusion of higher energies did not alter the yield ratio or the percent decomposition results. Examination of the product  $k_i \bar{N}_i$  showed little contribution to the overall decomposition arising from the highest energy levels.

Yield ratios were computed by using eq 17 and the percent decomposition was found by summing the numerator and the denominator of eq 17 and multiplying by  $\langle n \rangle / m$ , the fraction of excited molecules in the total population.

The three values of  $\langle n \rangle$  listed in Tables II and III represent the most reliable experimental values. In table II, the corresponding  $m$  values were obtained by using the desired  $\langle n \rangle / m$  ratio. Other  $m$  values were selected as those integers most consistent with the listed  $\langle n \rangle$ . The average energies listed in Table III are the  $m$  values, fixed by the selected  $\langle n \rangle / m$  ratios, multiplied by the photon energy, 1073 cm<sup>-1</sup>.

## Reliability of Bromide Ion Selective Electrodes for Studying the Oscillatory Belousov-Zhabotinsky Reaction<sup>1</sup>

N. Ganapathisubramanian and Richard M. Noyes\*

Department of Chemistry, University of Oregon, Eugene, Oregon 97403 (Received: January 28, 1982; In Final Form: April 28, 1982)

If either Ag<sup>+</sup> or Br<sup>-</sup> is added to an inert supporting electrolyte, the potential of a bromide ion selective electrode is in quantitative ( $\pm 1$  mV) agreement with prediction. Response time of the electrode is usually less than 1 min and often only a few seconds. If Br<sub>2</sub> is also present, rapid equilibria forming Br<sub>3</sub><sup>-</sup> and HOBr must also be considered; however, the electrode potential is still a valid measure of bromide ion activity at least above about 10<sup>-7</sup> M. If an excess of BrO<sub>3</sub><sup>-</sup> is present in an acidic medium, the equilibrium concentration of bromide is so low that the electrode would be seriously corroded if the AgBr surface were not protected by a boundary layer in which diffusion is slow. Such an electrode may reach a stable potential consistent with a bromide concentration orders of magnitude larger than that in the bulk solution. We conclude that simple extrapolation by means of the Nernst equation provides a satisfactory measure of bromide concentrations greater than a few times 10<sup>-7</sup> M, but minimum concentrations during Belousov-Zhabotinsky oscillations may be 2 or 3 orders of magnitude smaller than those calculated from the Nernst equation. This revised interpretation generates even better consistency than before between experimental observations and attempts to model the reaction numerically.

### Introduction

When Professor Endre Körös of Budapest came to Eugene in 1970 and saw the Belousov<sup>2</sup>-Zhabotinsky<sup>3</sup> os-

illating reaction, he suggested that we should study the behavior in it of an electrode specific to bromide ion. This prescient suggestion was the key factor that permitted the mechanism of the reaction to be unraveled.<sup>4</sup>

(1) No. 48 in the series "Chemical Oscillations and Instabilities". No 47 is: Noyes, R. M. "Nonlinear Phenomena in Chemical Dynamics"; Vidal, C., Pacault, A., Eds.; Springer-Verlag: West Berlin, 1981; pp 201-6.

(2) Belousov, B. P. *Ref. Radiat. Med.* 1959, 1958, 145-7.

(3) Zhabotinsky, A. M. *Dokl. Akad. Nauk SSSR* 1964, 157, 392-5.